Numerical investigation of supercontinuum generation and optical frequency combs in SiN-based PCF with high nonlinear coefficient*

Mohammad Reza Alizadeh[1], Mahmood Seifouri[1], and Saeed Olyaee[2]**

1. Faculty of Electrical Engineering, Shahid Rajaee Teacher Training University, Tehran, Iran

2. Nano-photonics and Optoelectronics Research Laboratory (NORLab), Shahid Rajaee Teacher Training University, Tehran, Iran

(Received 20 May 2023; Revised 9 August 2023)

In this paper, a photonic crystal fiber (PCF) with a dispersion-engineered and high nonlinear coefficient has been designed for supercontinuum generation (SCG) and frequency comb generation (FCG). The proposed PCF has a Si_3N_4 rod in the core. This rod provides more optical confinement in the core by increasing the refractive index of the core. This high confinement reduces the effective mode area of PCF and thus increases the nonlinear coefficient. The effective mod area and the nonlinear coefficient are obtained as 0.814 μm^2 and 25 $W^{-1}m^{-1}$, respectively. By varying different parameters for dispersion engineering, a suitable dispersion profile for the structure has been obtained so that the proposed PCF has two zero dispersion wavelengths (ZDWs) at 900 nm and 1 590 nm. By injecting a pumping with power of 1 kW and duration of 50 fs at a wavelength of 1 555 nm to the designed PCF with a length of 4 mm, the output spectrum is broadened in the range from 800 nm to 3 500 nm. For FCG by the four-wave mixing (FWM) method, phase matching conditions must be provided, and for that, the pumped wavelength must be in the anomalous dispersion regime and near ZDW. As a result, two continuous wave lasers pumping at the wavelengths of 1 551 nm and 1 558 nm have been injected into the PCF and optical frequency combs (OFCs) with a pulse width of 1 nm and a free spectral range of 7 nm has been obtained.

Document code: A **Article ID:** 1673-1905(2024)03-0163-8

DOI https://doi.org/10.1007/s11801-024-3092-7

In recent years, photonic crystal fibers (PCFs) have received a lot of attention due to their various applications. Different configurations of PCFs have been studied, including a type composed of silica with air holes and other PCFs incorporating composite materials in either the core or the holes[1]. PCFs have attracted significant attention due to their exceptional flexibility in manipulating various optical characteristics like dispersion, nonlinear effects, effective mode area, and other parameters. These fibers can manipulate these properties by altering the configuration or dimensions of air holes (d), and pitch (Λ), adjusting their shape, or employing different materials[2]. PCFs have various applications. As an important example, we can mention supercontinuum generation (SCG) and optical frequency comb (OFC) based on SCG[3]. Increasing the contrast of the refractive index between the core and the cladding causes the light to be confined in a smaller area in the core, and as a result, the nonlinear coefficient increases. The high nonlinear coefficient is a very important parameter in the case of SCG, so if the nonlinear coefficient is high enough, the required power for SCG is reduced. This feature makes PCFs very suitable and interesting for SCG.

The supercontinuum spectrum and OFCs have various applications, including tomography[4], optical metrology[5], frequency conversion[6], and spectroscopy[7]. So far, extensive research has been done to investigate and describe the mechanisms of supercontinuum spectral broadening[8-12]. One way to achieve SCG is by utilizing ultra-short pulses, typically in the femtosecond or picosecond range, and injecting them into a highly nonlinear PCF operating in the anomalous dispersion regime and near-zero dispersion wavelength. In these conditions, various nonlinear effects such as four-wave mixing (FWM), self-phase modulation (SPM), stimulated Raman scattering (SRS), and frequency instability appear along with high dispersion orders. Their interaction causes the input pulse to broaden and generate the supercontinuum spectrum. In order to use the supercontinuum spectrum in optical communication, a low-noise and stable spectrum is needed. In this case, the pumping pulse must be injected in the normal dispersion region,

* This work has been supported by Shahid Rajaee Teacher Training University (No.4976).

** E-mail: s_olyaee@sru.ac.ir

resulting in coherent SCG. In this case, the main nonlinear effects are SPM, cross-phase modulation, SRS, and FWM[13]. Also, to achieve a flatter spectrum, the use of PCF with two ZDWs or the use of dual pumping with different wavelengths is suggested[14]. In addition, dispersion and nonlinear effects can be engineered using filled liquids[15].

One of the important advantages of PCFs is the ability to control dispersion by modifying the size of their air holes. Additionally, it is possible to alter the dimensions in a manner that maximizes optical confinement and improves the nonlinearity of the PCF. For SCG, the use of nonlinear structures is very important and interesting. In this regard, materials with different nonlinear coefficients such as chalcogenide glasses[15] and III-V materials[16] have been used. These materials are not an appropriate complement to compact electronic and photonic circuits due to their incompatibility with CMOS. Silicon photonic circuits offer a potential solution to solve this issue. Silicon possesses both a high linear and nonlinear refractive index, making it suitable for constructing structures capable of SCG[17]. However, silicon has a high two-photon absorption (TPA) in the near-infrared wavelength range, which limits its use[18]. Structures based on silicon nitride (Si_xN_y) are compatible with silicon technology, and its TPA is negligible in the infrared wavelength range and has a nonlinear coefficient 10 times higher than silicon dioxide[18].

This study focuses on developing a PCF by incorporating a core material that has a high refractive index. The main goal is to confine the optical mode within the core, which leads to the reduction of the effective mode area. For this purpose, we have used a silica PCF with Si_3N_4 rod in the core. In this condition, the nonlinear coefficient is increased.

In this section, we examine the proposed PCF design and explore its different optical properties.

As mentioned, increasing the refractive index within the core causes light to be more confined in the core, which makes the PCF to be single-mode in a wide range of wavelength. As a result, the effective mode area decreases, and the nonlinear coefficient increases. Therefore, our intention is to utilize a rod in the core of the proposed fiber that possesses a significantly high refractive index. Fig.1(a) provides a visual representation of the PCF design. To increase the refractive index of the core, Si_3N_4 material is used, where its linear and nonlinear refractive index is higher than silica and shows better transparency in longer wavelengths. This fiber is a hexagonal PCF structure with 5 rings and the central ring has been removed. A Si_3N_4 rod is embedded in the core of PCF. In the proposed PCF, the refractive index of the core is high enough, which provides the conditions for the PCF to become single mode, while simultaneously providing a smaller effective mode area. The mode propagation profile of the proposed PCF can be seen in Fig.1(b).

In order to obtain the optimal structure, we first investigate the effect of different PCF parameters on the dispersion profile. The effect of lattice constant (a) on dispersion can be seen in Fig.2. As evident from this figure, with the increase of a, in addition to decreasing the flatness of the splash dispersion, it changes towards the normal dispersion regime. Also, with a further reduction of the lattice constant, the profile becomes flatter but increases in the anomalous regime.

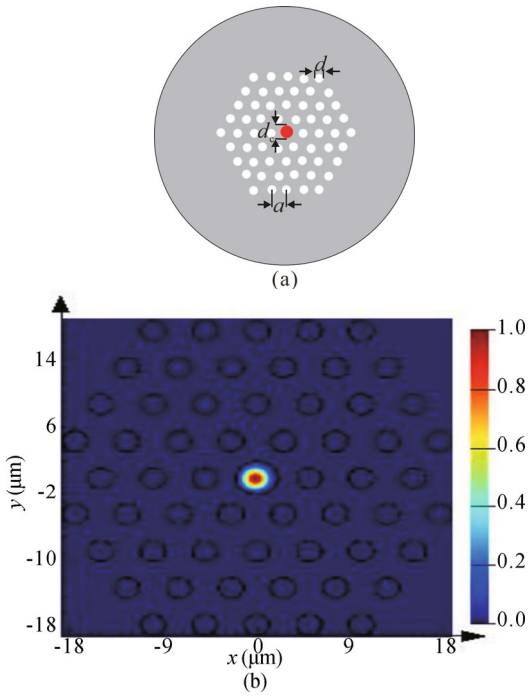

Fig.1 (a) The cross section of the proposed PCF; (b) The mode propagation profile of the proposed PCF

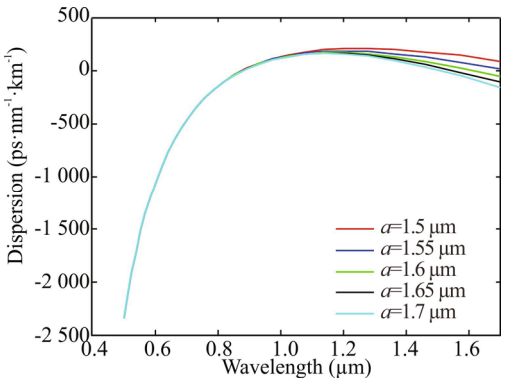

Fig.2 Variation of the dispersion curve in response to different lattice constants

Fig.3 displays the dispersion profile resulting from alterations in the radius (r) of the air holes. As the radius of the air holes has been increased, the profile has become flatter, but it increases in the anomalous dispersion regime. Also, its amount is increased in the anomalous regime. To generate a suitable SCG and desirable OFCs, an anomalous dispersion regime is needed, but the

amount of dispersion profile in this regime should be low and flat.

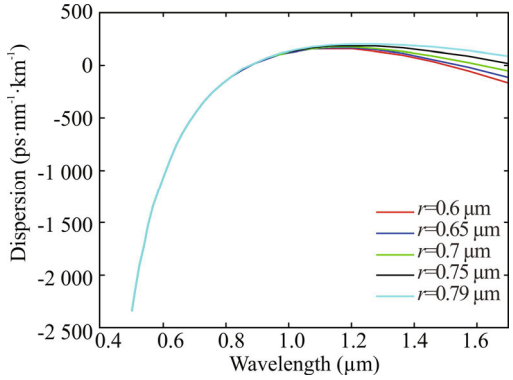

Fig.3 Variation of the dispersion curve in response to different air hole radii

As mentioned before, a Si_3N_4 rod has been used in the core to further confine the light in the core and increase the nonlinear coefficient. Fig.4 illustrates the impact of modifying the dimensions of the Si_3N_4 rod on the dispersion profile. When the radius of this rod is equal to 0.35 μm, the dispersion profile is completely in the normal regime. Although a normal dispersion regime is suitable for coherent and flat SCG, for phase matching to frequency comb generation (FCG) with the FWM method, an anomalous dispersion regime is needed, so the structure must be designed so that the dispersion curve has an anomalous part as well. As the radius of the rod increases, the dispersion moves toward the anomalous range. According to the mentioned discussion about PCF dimensions, finally, the values of these parameters have been set as a=1.6 μm, r=0.7 μm, and r_c=0.45 μm.

In this section, the SCG and OFC generation in the proposed PCF, whose optical properties were explained in the previous section, is investigated. The propagation of the optical signal in the optical fiber can be expressed by numerically solving the nonlinear Schrödinger equation. This equation is given as[18]

$$\frac{\partial}{\partial Z}A(Z,T)=-\frac{\alpha(\omega)}{2}A(Z,T)+\sum_{n\geq 2}\beta_n\frac{\mathrm{i}^{n+1}}{n!}\frac{\partial^n}{\partial t^n}A(Z,T)+$$

$$\mathrm{i}\gamma\left(1+\frac{\mathrm{i}}{\omega_0}\frac{\partial}{\partial t}\right)\int_{-\infty}^{+\infty}R(T')\left|A(Z,T-T')\right|^2\mathrm{d}T'', \quad (1)$$

where $A(Z, T)$ is the envelope of the input pulse, α is the loss coefficient, β_n is the nth order of dispersion at the central frequency ω_0 and $R(T)$ is the Raman response which is as follows[3]

$$R(T)=(1-f_r)\delta(T)+f_r h_r(T). \quad (2)$$

And the value of $h_r(T)$ is defined as

$$h_r(T)=\frac{\tau_1^2+\tau_2^2}{\tau_1\tau_2^2}\exp\left(\frac{-\tau}{\tau_2}\right)\sin\left(\frac{-\tau}{\tau_1}\right), \quad (3)$$

where τ_1, τ_2 and f_r have constant values and it is considered to be negligible in silicon nitride for Si_3N_4[18]. Schrödinger's equation can be solved simply and with high accuracy by the split-step Fourier method (SSFM).

According to the dimensions obtained for the proposed PCF in the previous section, the effective mode area is obtained as 0.814 μm^2. As a result, and according to the following equation, the nonlinear coefficient is 25 W^{-1}m^{-1}.

$$\gamma=\frac{2\pi}{\lambda}\frac{n_2}{A_{\mathrm{eff}}}. \quad (4)$$

Fig.5 shows the profile of the effective mode area and the nonlinear coefficient in terms of wavelength. As the wavelength increases, the effective mode area increases and according to Eq.(4), and the nonlinear coefficient decreases. Higher order dispersion values for the proposed PCF are calculated up to the 10th order and presented in Tab.1. Considering that dispersion plays an important role in the formation of the output spectrum, the calculation of these high-order terms enhances the accuracy of the calculations. To a broad SCG, it is useful to inject the pulse in the anomalous dispersion regime and near-to-zero dispersion wavelength[18]. According to the dispersion profile obtained in the previous section, the proposed structure has two ZDWs at 900 nm and 1 590 nm. Here we injected a 1 545 nm pump pulse into the PCF and near the second ZDW. Also, the input pulse power and duration are 600 W and 50 fs, respectively. The amount of loss in silicon in the mid-infrared range can be neglected, especially in applications where the required length is small, however, we set the amount of loss to 0.5 dB/cm[19]. The coupling loss between the optical source and the PCF is estimated to be 1.80 dB[19]. The broadening of the output SCG occurs as a result of the interaction between the effects associated with Eq.(1) when the input pumping is applied.

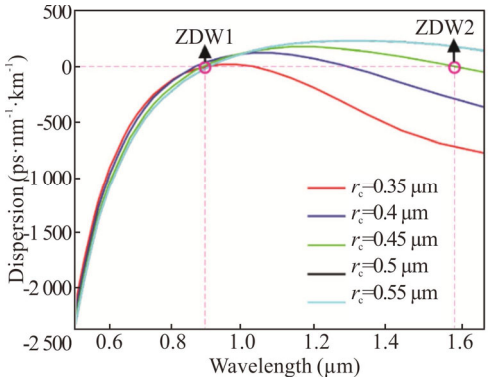

Fig.4 Variation of the dispersion curve in response to different Si_3N_4 rod radii

As the pulse propagates through the PCF, various nonlinear effects like frequency instability and SPM lead to the initial broadening of the spectrum. Subsequently,

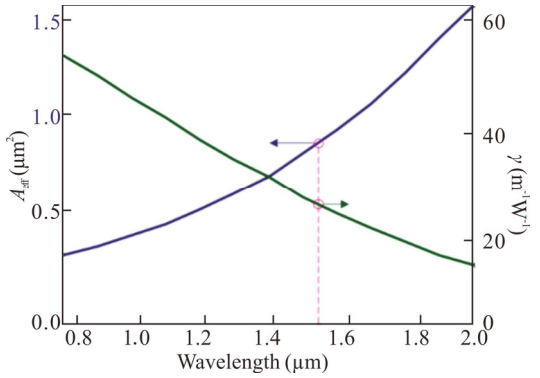

Fig.5 The nonlinear coefficient and the effective mode area versus wavelength

soliton fission takes place, resulting in the generation of new frequency components. Then, the SRS, FWM, phase matching, and other nonlinear effects make the spectrum broader. By injecting the mentioned pulse into the designed PCF with a length of 4 mm, a supercontinuum spectrum is obtained in the range from 800 nm to 3 500 nm. As shown in Fig.6, the spectral evolution and temporal evolution profiles are presented along the propagation length. It is evident from this figure that the process of generating SC through pumping in the anomalous dispersion regime results in temporal compression of solitons, accompanied by a symmetric broadening of the spectrum. As a consequence, a dispersive wave is generated at higher wavelengths.

Tab.1 Higher order dispersion values of the proposed PCF

β_n	β_2 (s^2/m)	β_3 (s^3/m)	β_4 (s^4/m)	β_5 (s^5/m)	β_6 (s^6/m)	β_7 (s^7/m)	β_8 (s^8/m)	β_9 (s^9/m)	β_{10} (s^{10}/m)
Value	-2.94×10^{-26}	2.8×10^{-39}	-2.71×10^{-54}	-9.6×10^{-69}	2.09×10^{-82}	-1.87×10^{-96}	4.82×10^{-110}	-1.21×10^{-123}	1.12×10^{-137}

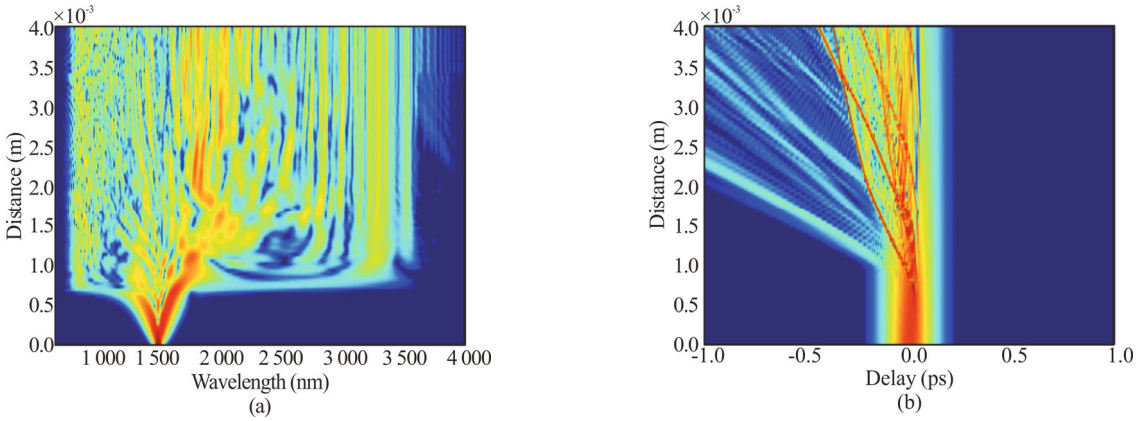

Fig.6 (a) Spectral evolution and (b) temporal evolution plots of the pulse versus propagation distance in the proposed PCF

The process of SPM results in the symmetrical broadening of the spectrum centered on the wavelength at which the pumping occurs. This means that the soliton is propagated through time compression processes. At a PCF length of approximately 0.55 mm, soliton fission gives rise to new frequency components across a relatively broad range. Almost at the same time as the soliton fission, the dispersive waves (DWs) are produced in wavelengths around 1 000 nm and 2 500 nm. Also, the Raman effect causes a shift to long wavelengths around the PCF length of 1 mm. In the same way, the trend of increasing the output intensity during the ZDW of the PCF is observed at 900 nm and 1 590 nm.

By broadening the spectrum in two additional sidebands, new frequency components emerge at wavelengths where dispersion is unfavorable, preventing efficient spectral broadening. To widen the spectrum, one can increase both the waveguide's length and the input pumping power. Furthermore, if the structure can be designed in such a way that the amount of dispersion in a wide range is low, flat, and close to zero, the output spectrum can be optimized in terms of width and coherence. Furthermore, the width of the input pulse is an additional crucial parameter that can impact the output spectrum, and this aspect will be further examined and discussed.

In Fig.7, the SCG in PCF lengths of 2 mm, 4 mm, and 8 mm is illustrated. At a propagation length of about 2 mm, a flat supercontinuum spectrum is obtained from 800 nm to 3 500 nm at the <−17 dB level. As the PCF length increases, this spectral width increases. As depicted in Fig.6, the effective spectrum broadening initially begins at 0.55 mm, and a suitable spectrum is obtained at the PCF length of 2 mm. Increasing the length of the PCF makes the further broadening of the output spectrum which can be seen in Fig.7. The result of this increase is the broadening of the spectrum in the normal dispersion regime, which gives a flat spectrum. Another effective factor in SCG is varying the input pulse width.

The result of varying the input pulse duration on the output spectrum is depicted in Fig.8. In this scenario, an input pulse with a power of 600 W at the wavelength of 1 545 nm is applied to the PCF in the anomalous dispersion regime. When the input pulse duration is 10 fs, the

spectrum has high flatness. When the width of the input pulse is extended, the resulting spectrum becomes less uniform and exhibits a reduced flatness. The decrease in flatness and uniformity of the output spectrum, along with the variations in intensity, are unfavorable for numerous applications.

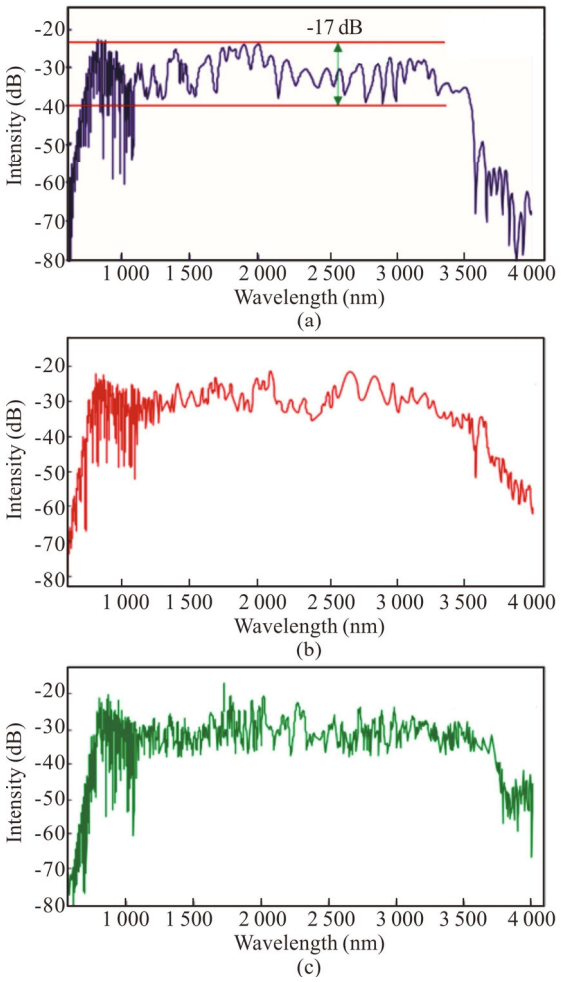

Fig.7 Impact of the length of the PCF on the output SCG: (a) *L*=2 mm; (b) *L*=4 mm; (c) *L*=8 mm

Although today with various techniques, it is not a serious challenge to produce pulses with a short width, suitable pulse widths such as 50 fs and above are more practical and available. Another important factor for SCG is the power of the input pulse. To investigate the effect of the input pulse power on the output spectrum, an input pump at a wavelength of 1 545 nm and a duration of 50 fs is utilized. Fig.9 illustrates that the results indicate an increase in the input power leading to the widening of the output spectrum as well. As either of these factors is increased, the resulting output spectrum becomes wider due to the increased involvement of nonlinear effects in the evolution of the pulse.

Tab.2 shows a comparison of the distinctive characteristics of the suggested setup and its discoveries in relation to previous studies conducted in this area. As mentioned, applying an input pulse to the anomalous dispersion region results in a wide output spectrum. The proposed PCF is specifically designed to ensure that its ZDW falls within the range of telecommunication wavelengths to enable the FCG for telecommunication applications. While the spectral width of the proposed structure is comparable or, in some cases, lower than previous works, precise dispersion engineering has simultaneously enabled the necessary phase matching to generate frequency combs.

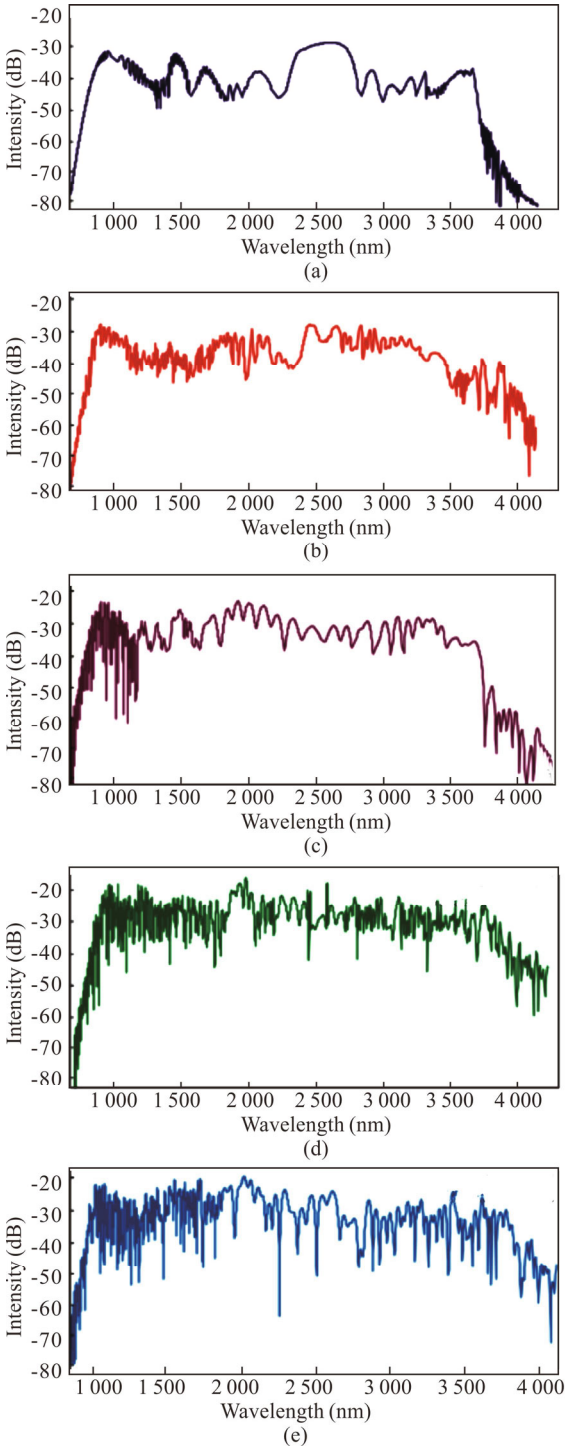

Fig.8 Impact of the input pulse duration on the SCG: (a) *FWHM*=10 fs; (b) *FWHM*=30 fs; (c) *FWHM*=50 fs; (d) *FWHM*=100 fs; (e) *FWHM*=200 fs

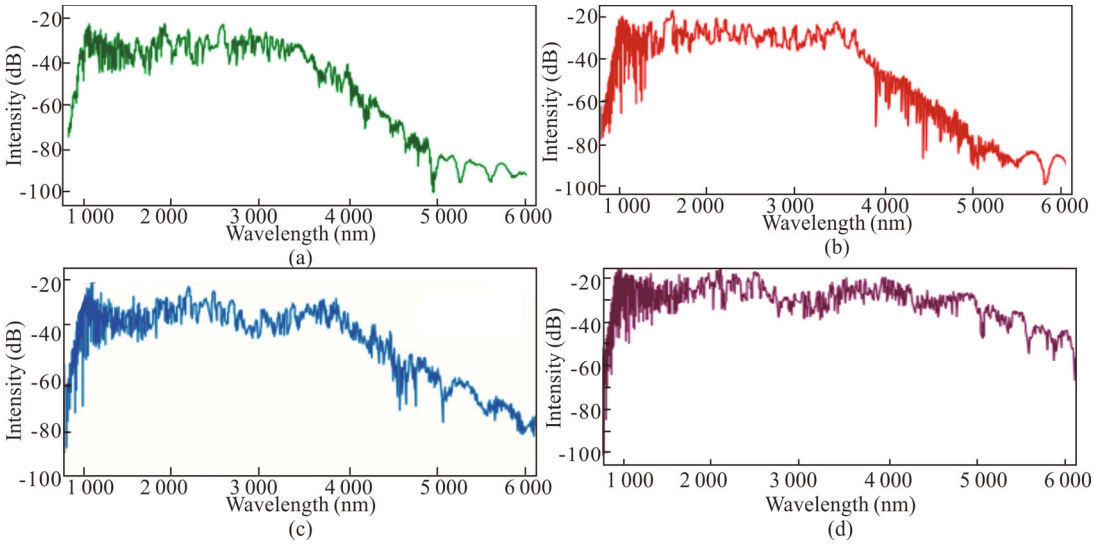

Fig.9 Impact of the power of input pulse on the SCG: (a) *P*=400 W; (b) *P*=600 W; (c) *P*=1 kW; (d) *P*=2 kW

Tab.2 Comparison of the properties and findings between the proposed PCF and prior research

References	Material	P_{in}	Pulse duration (fs)	λ_0 (nm)	Bandwidth (nm) (FCG)	Bandwidth (nm) (SCG)
[20]	$As_{38.8}Se_{61.2}$	0.88 kW	50	3 700	-	1 700
[21]	SOI	400 W	200	2 100	-	2 800
[22]	ZBLAN	1 110 kW	110	2 000	-	3 500
[23]	As_2Se_3	10 kW	50	4 600	-	3 860
[24]	Nitrobenzene	20 kW		1 560	1 300	-
[25]	Silica	720 W		1 550	-	1 100
[26]	ZBLAN	12.5 kW	10 000	1 550	-	3 500
[27]	$As_{40}Se_{60}$	50 kW	100	4 250	-	11 000
[28]	-	250 W		976	15	-
[29]	SiN	130 mW		1 550	56	-
This work	Si_3N_4	1 kW	50	1 555	150	2 700

In order to generate the OFC, two CW laser pumps are injected into the PCF at the wavelengths of 1 551 nm and 1 558 nm. Considering that these two wavelengths are near the ZDW, they create the essential conditions for phase matching, thereby enabling the generation of OFCs. Fig.10 shows the output OFC around the PCF length of 1 mm, which has a linewidth of 1 nm and a free spectral range of 7 nm. The number of comb lines is 16 in the range of 15 dBm. Here, we have used the FWM method to generate frequency combs. To ensure phase matching, the input power must be lower than the threshold of other effects such as stimulated Raman and Brillion effects. As a result, the input power here is considered to be 20 W, which results in the dominance of FWM.

As the power or length of the PCF increases, other effects gradually appear, and as a result, new frequency components are generated, which interact with the comb lines generated by FWM. Although in this case, the spectral width in the output increases, the extraction of frequency combs requires more complex structures. Here, it has been made to use a single PCF for the generation of frequency combs, eliminating the need for complicated designs. This approach facilitates compatibility with optical integrated circuits. A parallel structure with a shifted ZDW can be employed to enhance the bandwidth. By altering the ZDW, phase matching can be achieved within the intended spectral range. Furthermore, employing the FWM technique allows for adjusting the frequency spacing or wavelength of the frequency combs. Considering Ref.[30], the fabrication potential for the proposed PCF will be easily feasible. Also, from the viewpoint of PCF fabrication, the deviation of structural parameters from achieved values cannot be completely avoided. Consequently, a tolerance analysis for the performance of the proposed PCF is necessary. The main factor to determine the output spectrum

is the dispersion profile of the PCF, so the effect of structural parameters on the dispersion profile should be investigated. For this, the structural parameters (a, d, and d_c in Fig.1(a)) have been independently investigated by ±10% with respect to the optimal values and there was no discernible variation in the structure's dispersion profile and loss.

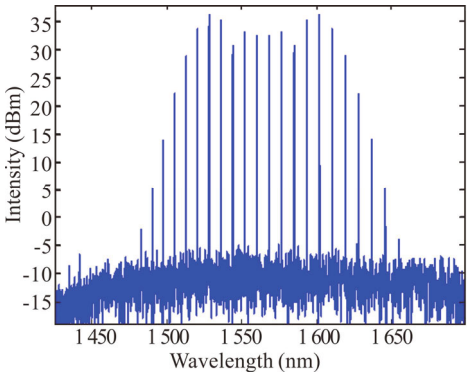

Fig.10 Output OFC of the proposed PCF

In this paper, a dispersion-engineered PCF with high nonlinear coefficient was designed to generate frequency combs. To increase the contrast between the refractive index of the core and the cladding, a Si_3N_4 rod was added to the core of PCF. Incorporating of this rod in the core of PCF caused more light confinement in the core, and as a result, the effective mode area decreased and the nonlinearity increased. The effective mod area was equal to 0.814 μm^2 and as a result, the nonlinear coefficient of PCF was obtained as 25 W^{-1}m^{-1}. By varying different parameters for dispersion engineering, a suitable dispersion profile for the structure was obtained. So, the structure has two ZDW at 900 nm and 1 590 nm. By injecting an input pulse at a wavelength of 1 545 nm and power of 600 W with a duration of 50 fs into the designed PCF with a length of 4 mm, a supercontinuum spectrum in the range from 800 nm to 3 500 nm was obtained. For FCG by the FWM method, phase matching conditions must be provided. As a result, two continuous wave laser pumps at wavelengths of 1 551 nm and 1 558 nm were injected into the PCF, and OFCs with a pulse width of 1 nm and free spectral range of 7 nm were obtained. This structure is suitable for optical communication, remote sensing applications, remote surgery, and similar operations.

Ethics declarations

Conflicts of interest

The authors declare no conflict of interest.

References

[1] JUN Q, SHU H W, CHANG L, et al. On-chip high-efficiency wavelength multicasting of PAM3/PAM4 signals using low-loss AlGaAs-on-insulator nanowaveguides[J]. Optics letters, 2020, 45(16): 4539-4542.

[2] WILLNER A E, FALLAHPOUR A, ALISHAHI F, et al. All-optical signal processing techniques for flexible networks[J]. Journal of lightwave technology, 2019, 37(1): 21-35.

[3] DUDLEY J M, GENTY G, COEN S. Supercontinuum generation in photonic crystal fiber[J]. Reviews of modern physics, 2006, 78(4): 1135-1184.

[4] BORGOHAIN N, SHARMA M, KONAR S. Broadband supercontinuum generation in photonic crystal fibers using cosh-Gaussian pulses at 835 nm wavelength[J]. Optik, 2016, 127(4): 1630-1634.

[5] DAI S X, WANG Y Y, PENG X F. Review of mid-infrared supercontinuum generation in chalcogenide glass fibers[J]. Applied science, 2018, 8(5): 707.

[6] SAFIOUI J. Supercontinuum generation in hydrogenated amorphous silicon waveguides at telecommunication wavelengths[J]. Optic express, 2014, 22: 3089-3097.

[7] LUO B H, WANG Y Y, DAI S X, et al. Midinfrared supercontinuum generation in As_2Se_3-As_2S_3 chalcogenide glass fiber with high NA[J]. Journal of lightwave technology, 2017, 35(12): 2464-2469.

[8] SEIFOURI M, OLYAEE S, KARAMI R. A new design of As_2Se_3 chalcogenide nanostructured photonic crystal fiber for the purpose of supercontinuum generation[J]. Current nanoscience, 2017, 13(2): 202-207.

[9] GHANBARI A, OLYAEE S. Highly nonlinear composite-photonic crystal fibers with simplified manufacturing process and efficient MID-IR applications[J]. Crystals, 2023, 13(2): 1-17.

[10] GHANBARI A, OLYAEE S. A computational method for simple design of endlessly all-silica large mode area photonic crystal fiber for high power laser applications[J]. Journal of computational electronics, 2023, 22(2): 704-715.

[11] CHESHMBERAH A, SEIFOURI M, OLYAEE S. Design of all-normal dispersion with $Ge_{11.5}As_{24}Se_{64.5}$/$Ge_{20}Sb_{15}Se_{65}$ chalcogenide PCF pumped at 1300 nm for supercontinuum generation[J]. Optical and quantum electronics, 2021, 53(8): 1-11.

[12] CHESHMBERAH A, SEIFOURI M, OLYAEE S. Supercontinuum generation in PCF with As_2S_3/$Ge_{20}Sb_{15}Se_{65}$ chalcogenide core pumped at second telecommunication wavelengths for WDM[J]. Optical and quantum electronics, 2020, 52(12): 1-14.

[13] HU H, OXENLØWE L K. Chip-based optical frequency combs for high-capacity optical communications[J]. Nanophotonics, 2021, 10(5): 1367-1385.

[14] BOUCON A, SYLVESTRE T, HUY K P, et al. Supercontinuum generation by nanosecond dual-pumping near the two zero-dispersion wavelengths of a photonic crystal fiber[J]. Optics communications, 2011, 284(1): 467-470.

[15] MONFARED Y E, PONOMARENKO S A. Extremely nonlinear carbon-disulfide-filled photonic crystal fiber with controllable dispersion[J]. Optical materials, 2019, 88: 406-411.

[16] YI D, WU C, LIU Y, et al. Dual-pumped flat optical

frequency comb based on normal dispersion AlGaAs on insulator waveguide: numerical investigation[J]. Optics communications, 2022, 502: 127415.

[17] CHILES J, NADER N, STANTON E J, et al. Multi-functional integrated photonics in the mid-infrared with suspended AlGaAs on silicon[J]. Optica, 2019, 6(9): 1246-1254.

[18] ALIZADEH M R, SEIFOURI M. Investigation of highly broadb and supercontinuum generation in a suspended As_2Se_3 based ridge waveguide[J]. Journal of optoelectronical nanostructures, 2020, 5(4): 1-16.

[19] XIAO L M, JIN W, DEMOKAN M S, et al. Photopolymer microtips for efficient light coupling between single-mode fibers and photonic crystal fibers[J]. Optics letters, 2006, 31: 1791-1793.

[20] MBAYE D, AMINE B S, RIM C, et al. Super-flat coherent supercontinuum source in $As_{38.8}Se_{61.2}$ chalcogenide photonic crystal fiber with all-normal dispersion engineering at a very low input energy[J]. Applied optics, 2017, 56: 163-169.

[21] HAMED S, VIEN V. Broadband mid-infrared supercontinuum generation in dispersion-engineered silicon-on-insulator waveguide[J]. Journal of the optical society of America B, 2019, 36: A193-A202.

[22] CHRISTIAN A, CHRISTIAN P, SUNE D, et al. Supercontinuum generation in ZBLAN fibers-detailed comparison between measurement and simulation[J]. Journal of the optical society of America B, 2012, 29: 635-645.

[23] HAMED S, MAJID E H, MOHAMMAD K M F. Mid-infrared supercontinuum generation via As_2Se_3 chalcogenide photonic crystal fibers[J]. Applied optics, 2015, 54: 2072-2079.

[24] GUO Y C, YUAN J H, WANG K R, et al. Generation of supercontinuum and frequency comb in a nitrobenzene-core photonic crystal fiber with all-normal dispersion profile[J]. Optics communications, 2021, 481(4): 126555.

[25] TARNOWSKI K, TADEUSZ M, PAWEŁ M, et al. Compact all-fiber source of coherent linearly polarized octaves panning supercontinuum based on normal dispersion silica fiber[J]. Scientific reports, 2019, 9: 12313.

[26] IRNIS K, CHRISTIAN S A, PETER M M, et al. Mid-infrared supercontinuum generation to 4.5 μm in uniform and tapered ZBLAN step-index fibers by direct pumping at 1064 or 1550 nm[J]. Journal of the optical society of America B, 2013, 30: 2743-2757.

[27] SAGHAEI H, MORAVVEJ-FARSHI M K, EBNALI-HEIDARI M, et al. Ultra-wide mid-infrared supercontinuum generation in $As_{40}Se_{60}$ chalcogenide fibers: solid core PCF versus SIF[J]. IEEE journal of selected topics in quantum electronics, 2016, 22(2): 279-286.

[28] NAUTA J, OELMANN J H, BORODIN A, et al. XUV frequency comb production with an astigmatism-compensated enhancement cavity[J]. Optics express, 2021, 29(2): 2624-2636.

[29] XIE Y Z, LI J Q, ZHANG Y F, et al. Soliton frequency comb generation in CMOS-compatible silicon nitride microresonators[J]. Photonics research, 2022, 10: 1290-1296.

[30] HE X T, LIANG E T, YUAN J J, et al. A silicon-on-insulator slab for topological valley transport[J]. Nature communications, 2019, 10: 872.